Journal of Sound and Vibration (1997) **202**(3), 361–373

DEVELOPMENT OF THE DIRECT BOUNDARY ELEMENT METHOD FOR THIN BODIES WITH GENERAL BOUNDARY CONDITIONS

K.-D. Ih and D.-J. Lee

Laboratory of Aerodynamics and Aeroacoustics, *Department of Aerospace Engineering*, *Korea Advanced Institute of Science and Technology*, 373-1, *Kusong-Dong Yusong-Ku*, 305-701, *Taejon*, *Korea*

(*Received* 28 *October* 1995; *and in final form* 27 *September* 1996)

A direct boundary element method (DBEM) is developed for thin bodies whose surfaces are rigid or compliant. The Helmholtz integral equation and its normal derivative integral equation are adopted simultaneously to calculate the pressure or the velocity potential *on both sides of thin body*, instead of the jump values across it, to account for the different surface conditions of each side. Unlike the usual assumption, the normal velocity is assumed to be discontinuous across the thin body. In this approach, only the neutral surface of the thin body has to be discretized. The method is validated by comparison with analytical and/or numerical results for acoustic scattering and radiation from the surface of a thin body under several conditions: when the surfaces are rigid while stationary or vibrating, and when part of the interior is lined with a sound absorbing material.

1. INTRODUCTION

Studies show that the conventional boundary element method (BEM) using the Helmholtz integral equation fails to yield reliable results for thin bodies. The major reason for this failure is that the integral is nearly singular, owing to the mesh on one side of the thin body being too close to the mesh on the opposite side.

Seybert *et al*. [1] adopted a multi-domain BEM formulation for the thin-body acoustic problem in which a fictitious interface surface is constructed to divide the acoustic field into several subdomains. By this means, the Helmholtz integral equation for a fictitious thick body enclosed by the thin-body surface and the fictitious surface can be solved in a straightforward manner. While the concept of the multi-domain BEM is simple, construction of the mesh in preprocessing is laborious, and it also results in a very large system of equations if the fictitious surface is relatively large.

Martinez [2] defined the failure as a thin-shape breakdown (TSB) and showed by a systematic analysis that an approach based on a normal derivative of the Helmholtz integral equation provides a robust formulation for a thin body. Applied to a rigid wall or a state of continuous oscillation, it leads to neither TSB nor non-unique solutions. However, the normal derivative integral equation has a hypersingular integral of the order of $O(1/r^3)$ the regularization of which requires a special technique.

In a direct boundary element method (DBEM) approach, Wu and Wan [3] proved that the same failure problem cannot be solved by DBEM because the Helmholtz integral equation becomes degenerate. They solved the normal derivative integral equation formulation for the thin body with a less singular normal derivative integral equation,

0022–460X/97/180361 + 13 $25.00/0/sv960829

derived by Maue [4] and later by Mitzner [5]. Detailed discussion of the regularization of the hypersingular integral is summarized in [6]. Wu and Wan used regular C^0 isoparametric elements with collocation points inside each element. In the derivation they initially constructed an imaginary interface surface to divide the acoustic domain into an interior and an exterior subdomain, as in the multi-domain BEM. Adding the Helmholtz integral equations and the normal derivative integral equations for each subdomain respectively, they obtained a combined Helmholtz integral equation and a combined normal derivative integral equation, which require discretization of the real surface only. A condition of continuity of normal velocity across the thin body is generally assumed *a priori*, due to the material homogeneity across the thickness of the thin body.

Recently, the method was applied to a regular body with thin fins and a vibrating surface by solving a mixed thin-body and regular-body integral formulation [7], which showed good agreement with the multi-domain BEM solution. The assumption of continuous normal velocity across the thin body is not often compatible when (1) either side of the thin body is mounted with different materials, or (2) either side of the thin body vibrates in a different manner. Because of the primary assumption of normal velocity continuity, the methods in [3, 7] cannot be applied to a thin body having different materials and/or different velocity conditions on each side.

In addition to the above mentioned works, different approaches have been carried out for the thin-body problem. Hamdi and Ville [8] and Wu *et al*. [9] used a variational formulation to avoid the evaluation of the hypersingular integral, but at the cost of evaluating a double surface integral. Malbéqui *et al*. [10] used an indirect boundary element method (IDBEM) for a duct, which was assumed to be hard-walled both inside and outside. Martinez, using a modal boundary integral technique, analyzed the acoustic diffraction due to a sound source by an open-ended cylindrical duct, where the interior surface of the duct was rigid [11] and/or with a compliant lining [12]. For a compliant boundary, Seybert *et al*. [1] calculated the acoustic radiation from a source within a partial enclosure. The calculation was carried out using the multi-domain BEM for the cases when both the inside and outside of the enclosure was rigid, and when the interior surfaces were lined with a sound-absorbing material. However, treatment of the thin-body problem with a compliant lining by using DBEM for the normal derivative integral equation formulation was not reported.

In this paper, a new DBEM is formulated to extend to thin bodies with rigid and compliant surfaces using the combined Helmholtz integral equation and the combined normal derivative integral equation. This can be done by removing the normal velocity continuity assumption across the thin body. In the formulation, the primary variables in the integral equation are the velocity potential (or pressure) jump for the rigid surface, and the normal velocity jump across the thin-body surface of different materials (or normal vibrating velocities). The normal velocity on each surface can be transformed into the velocity potential on each side by the prescribed acoustic admittance and the prescribed vibrating velocity, that is, by the general boundary conditions. Thus, the velocity potential values on each surface become unknowns, and the combined Helmholtz integral equation and combined normal derivative integral equation are solved simultaneously.

The hypersingular integral is regularized by using Maue's less singular normal derivative integral equation. It is reported that Maue's equation converges in the Cauchy principal value sense, rather than only in the finite part sense [3, 13]. Hence, the numerical integration can be carried out using a standard Gaussian quadrature. The collocation points are at the nodal points for the combined Helmholtz integral equation and inside each element for the combined normal derivative integral equation to confirm the

condition at the corner and the vertex. The knife-edge effect is treated by adopting quarter-point elements [14–16].

The selected benchmark problems are plane-wave scattering by a circular disk and the acoustic radiation from a vibrating circular disk. The present results for thin bodies are compared with the analytical solutions. Scattering from a cylindrical shell open at one side is calculated and compared with the result obtained by Wu and Wan [3] to check the solid angle effect at the corners and vertexes. Finally, we calculate the plane wave scattering by a cylindrical shell with one side open and a partly compliant lining at the bottom, and compare this with the result obtained using the multi-domain BEM.

2. INTEGRAL FORMULATION FOR THE THIN BODY COATED IN DIFFERENT MATERIALS

Figure 1 depicts the mathematical notations for a thin body coated in different materials on each side in a homogeneous acoustic medium. The acoustic field is temporarily divided into two parts (the exterior subdomain Ω^+ and the interior subdomain Ω^- by an imaginary surface, s, to formulate a new integral equation for the thin body [1, 3]. The thin body is mathematically described by a neutral surface, S, because the surface exposed to each subdomain is assumed to be coated in a different material. The velocity potential in the subdomain Ω^- is denoted by ϕ^-, the velocity potential in Ω^+ is ϕ^+ and the acoustic source is ϕ_{Sc}. The velocity potential is defined as $\vec{v} = -\nabla\phi$ and the $e^{+i\omega t}$ convention for time harmonic analysis is used. Then, the acoustic pressure can be calculated by $p = ik\rho_0 a_0 \phi$, where $i = \sqrt{-1}$, $k = \omega/a_0$ is the wave number, ρ_0 is the density of acoustic medium and a_0 is the speed of sound. The surface normal unit vector, $\hat{\mathbf{n}}$, is taken toward the exterior subdomain Ω^+.

By applying Green's theorem to the Helmholtz equation, the Helmholtz integral equation for each subdomain is obtained as shown below:

$$C^+(P)\phi^+(P) = -\int_{S+s} G(P, Q)\frac{\partial\phi^+(Q)}{\partial n} - \frac{\partial G(P, Q)}{\partial n}\phi^+(Q)\,\mathrm{d}S(Q) \tag{1}$$

and

$$C^-(P)\phi^-(P) = +\int_{S+s} G(P, Q)\frac{\partial\phi^-(Q)}{\partial n} - \frac{\partial G(P, Q)}{\partial n}\phi^-(Q)\,\mathrm{d}S(Q) + 4\pi\phi_{Sc}(P, X_{Sc}) \tag{2}$$

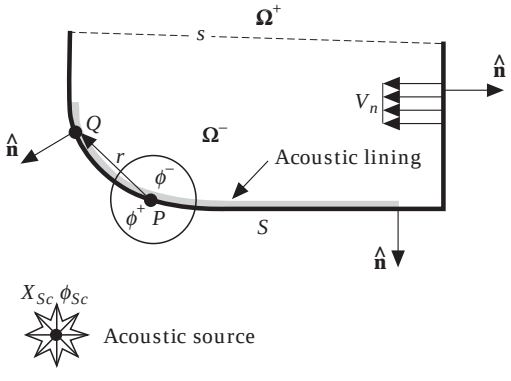

Figure 1. Mathematical model for a thin-body coated in different materials.

where P is the collocation point, Q is the secondary source point on the surface and X_{Sc} is the acoustic source point. The surface integral is applied to $S + s$. The symbols C^-, C^+ represent the solid angles at P in the exterior and interior subdomains respectively. The kernel function $G(P, Q)$ is the free-space Green's function, $G(P, Q) = e^{-ikr}/r$, in which $r = |Q - P|$.

Adding equation (1) and equation (2) results in a single equation (the combined Helmholtz integral equation):

$$C^+(P)\phi^+(P) + C^-(P)\phi^-(P) = -\int_S G(P, Q)\left(\frac{\partial\phi^+(Q)}{\partial n} - \frac{\partial\phi^-(Q)}{\partial n}\right) dS(Q)$$

$$+ \int_S \frac{\partial G(P, Q)}{\partial n}\,(\phi^+(Q) - \phi^-(Q))\, dS(Q)$$

$$+ 4\pi\phi_{Sc}(P, X_{Sc}). \tag{3}$$

The first part of the right side, usually deleted for the rigid surface because of the continuous normal velocity, is included in the above equation. The integrations on the fictitious surface are canceled because of the continuity of pressure (or velocity potential) and particle velocity on that surface.

By taking the normal derivative to equation (3), another combined normal derivative integral equation is obtained:

$$C^+(P)\frac{\partial\phi^+(P)}{\partial n_p} + C^-(P)\frac{\partial\phi^-(P)}{\partial n_p} = -\int_S \frac{\partial G(P, Q)}{\partial n_p}\left(\frac{\partial\phi^+(Q)}{\partial n} - \frac{\partial\phi^-(Q)}{\partial n}\right) dS(Q)$$

$$+ \int_S \frac{\partial^2 G(P, Q)}{\partial n_p\,\partial n}\,(\phi^+(Q) - \phi^-(Q))\, dS(Q)$$

$$+ 4\pi\,\frac{\partial\phi_{Sc}(P, X_{Sc})}{\partial n_p}\,. \tag{4}$$

In a typical thin-body radiation or scattering problem, the normal velocity, $\partial\phi/\partial n$, is generally assumed to be continuous across the thin body, as mentioned before. However, in the case of the thin body having different impedance (or admittance) on each side, the normal velocity on each side is different. So, in addition to the pressure jump between both surfaces of the thin body, a jump in normal velocity also exists.

From equations (3) and (4), four unknowns, $\partial\phi^\pm/\partial n$, $\phi^\pm$, are to be determined. Thus, to solve the acoustic field, two additional equations or conditions are necessary. Two conditions can be obtained from the boundary conditions. The general boundary conditions on both sides are given by:

$$\partial\phi^+/\partial n = -\alpha^+\phi^+ - \beta^+ \qquad \text{and} \qquad \partial\phi^-/\partial n = \alpha^-\phi^- + \beta^-, \tag{5a, 5b}$$

where $\alpha^\pm = i\rho_0 a_0 k Y^\pm$ are coefficients related to the acoustic admittance ($Y^\pm$) and $\beta^\pm$ are normal vibration velocities on each side of the thin-body surface. Sound-absorbing materials may be divided into two groups based on their characteristics [17], that is,

locally-reacting and bulk-reacting materials. In this paper, the former is assumed and is characterized by a normal acoustic impedance valid at the material surface.

Special conditions to treat the diffraction effect at the knife-edge are:

$$\phi^+ = \phi^-. \tag{5c}$$

Physically, this condition illustrates that the pressure is continuous along the edge.

After applying the boundary conditions, equation (5a) and (5b), to equations (3) and (4), two integral equations with two unknowns ϕ^+ and ϕ^- on the surface can be deduced as:

$$\begin{aligned} C^+\phi^+(P) + C^-\phi^-(P) = & \int_S \left(\alpha^+ G(P, Q) + \frac{\partial G(P, Q)}{\partial n}\right)\phi^+(Q)\,\mathrm{d}S(Q) \\ & + \int_S \left(\alpha^- G(P, Q) - \frac{\partial G(P, Q)}{\partial n}\right)\phi^-(Q)\,\mathrm{d}S(Q) \\ & + \int_S (\beta^+ + \beta^-)G(P, Q)\,\mathrm{d}S(Q) + 4\pi\phi_{Sc}(P, X_{Sc}) \end{aligned} \tag{6}$$

and

$$\begin{aligned} 2\pi\alpha^+\phi^+(P) - 2\pi\alpha^-\phi^-(P) = & \int_S \left(\alpha^+ \frac{\partial G(P, Q)}{\partial n_p} + \frac{\partial^2 G(P, Q)}{\partial n_p \partial n}\right)\phi^+(Q)\,\mathrm{d}S(Q) \\ & + \int_S \left(\alpha^- \frac{\partial G(P, Q)}{\partial n_p} - \frac{\partial^2 G(P, Q)}{\partial n_p \partial n}\right)\phi^-(Q)\,\mathrm{d}S(Q) \\ & + \int_S (\beta^+ + \beta^-)\frac{\partial G(P, Q)}{\partial n_p}\,\mathrm{d}S(Q) \\ & + 4\pi\frac{\partial \phi_{Sc}(P, X_{Sc})}{\partial n_p} + 2\pi(\beta^+ - \beta^-). \end{aligned} \tag{7}$$

The collocation point in equation (7) is selected to sustain the C^1 continuity of pressure [3, 13]. The solid angles on both sides (C^+, C^-) are 2π. Hence, one can obtain velocity potentials on both sides of the thin body by solving equations (6) and (7) simultaneously.

After finding out the values on the thin-body surface, the acoustic field at any point can be obtained by integrating equation (3) with the boundary conditions, equations (5a) and (5b). The values on the thin-body surface can be obtained by solving equations (6) and (7). Then, the acoustic field at any point can be obtained by integrating equation (3). Note that in this method, unlike that of Wu and Wan [3], it is not necessary to divide the jump value of velocity potential into the values inside and outside relative to each side of the thin body.

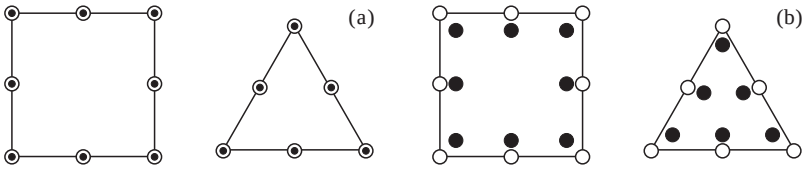

Figure 2. Configuration of the master elements. (a) master elements for equation (6); (b) master elements for equation (7). (hollow circle: nodal points; flooded circle: collocation points).

3. TREATMENT OF PROBLEMS IN THE INTEGRAL EQUATION

It is well known that the integration has the following problems: the integration of the singular kernel, the treatment of singularity near the knife edge, the non-uniqueness of the solution, and the treatment of the corner and the vertex. The following approaches were adopted to solve these integration problems.

First, the kernel $\partial^2 G/\partial n_p \partial n$ is hypersingular in the order of $O(1/r^3)$, so that an acceptable result cannot be obtained in this case. Thus, it is essential to reduce the order of singularity. Putting collocation points inside each element satisfies the C^1 continuity condition and makes it possible to use the following important relation derived by Maue [4] and later by Mitzner [5]:

$$\int_S \frac{\partial^2 G}{\partial n_p \partial n}\,\phi \,\mathrm{d}S = \int_S [\hat{\mathbf{n}}_p \times \nabla_p G) \cdot (\hat{\mathbf{n}} \times \nabla \phi) + k^2 (\hat{\mathbf{n}}_p \cdot \hat{\mathbf{n}}) G\phi]\,\mathrm{d}S. \tag{8}$$

The order of singularity then becomes $O(1/r^2)$, and adopting local polar co-ordinates further reduces the order of singularity to $O(1/r)$. Now, the standard Gaussian quadrature can be applied to the reduced integration. In this paper, the singular integration is carried out using the method in [13], based on Cauchy principal integration.

Second, the acoustic velocity potential has a singularity at the knife edge in the order of $O(1/\sqrt{r})$. Even using a fine mesh of higher-order elements will not produce sufficient accuracy, but by using node-shift elements or quarter-point elements, the knife edge singularity can be overcome easily [3, 15, 16].

Third, the non-uniqueness problem (occurring at some frequencies related to the eigenvalues of the corresponding interior region of the body) is not severe in the thin body case. The number of eigenvalues for a particular geometry is given approximately as:

$$n_{eigen} = Vk^3/6\pi^2, \tag{9}$$

where V is the volume of the body. For a thin body, V is zero, so it is not necessary to consider the non-uniqueness problem in this case [7].

The final problem is how to treat the solid-angle effect at the corner or the vertex. Collocation points that are placed inside the elements cannot represent the solid angles at the corners or vertices, and since the solid angle is defined at a point, such approximations as interpolation and extrapolation are not good treatments. Therefore, two kinds of collocation points on each element are used: for equation (6), collocation points are placed on the boundary of the element to calculate the correct solid angle, while for equation (7), as mentioned before, collocation points are placed inside the elements to use equation (8). The configurations of the master elements for equations (6) and (7) are shown in Figure 2.

4. NUMERICAL IMPLEMENTATION

An isoparametric eight-node quadrilateral and a six-node triangular element is used in this paper. The co-ordinate and the physical quantities on the surface are approximated by those at nodal points; that is:

$$x_i(\vec{\xi}) = \sum_{\alpha} N_\alpha(\vec{\xi}) X_{i\alpha} (i = 1, 2, 3); \qquad \phi(\vec{\xi}) = \sum_{\alpha} N_\alpha(\vec{\xi}) \Phi_\alpha (\alpha = 1, 2, \ldots, 6 \text{ or } 8), \tag{10}$$

where $N_\alpha(\vec{\xi})$ is the quadratic shape function and $X_{i\alpha}$, Φ_α are nodal quantities. Thus, a system equation can be deduced from equations (6) and (7):

$$\begin{bmatrix} A_{++} & A_{+-} \\ A_{-+} & A_{--} \end{bmatrix} \begin{Bmatrix} \Phi^+ \\ \Phi^- \end{Bmatrix} = \begin{Bmatrix} F_+ \\ F_- \end{Bmatrix}. \tag{11}$$

Components in the matrix are defined as follows:

$$A_{++} = -\int_{S_m} \left[\alpha^+(Q(\vec{\xi})) G(P, Q(\vec{\xi})) + \frac{\partial G(P, Q(\vec{\xi}))}{\partial n} \right] N(\vec{\xi})\, \mathrm{d}S_m, \tag{12a}$$

$$A_{+-} = -\int_{S_m} \left[\alpha^-(Q(\vec{\xi})) G(P, Q(\vec{\xi})) - \frac{\partial G(P, Q(\vec{\xi}))}{\partial n} \right] N(\vec{\xi})\, \mathrm{d}S_m, \tag{12b}$$

$$A_{-+} = -\int_{S_m} \left[\alpha^+(Q(\vec{\xi})) \frac{\partial G(P, Q(\vec{\xi}))}{\partial n_p} + \frac{\partial^2 G(P, Q(\vec{\xi}))}{\partial n\, \partial n_p} \right] N(\vec{\xi})\, \mathrm{d}S_m, \tag{12c}$$

$$A_{--} = -\int_{S_m} \left[\alpha^-(Q(\vec{\xi})) \frac{\partial G(P, Q(\vec{\xi}))}{\partial n_p} - \frac{\partial^2 G(P, Q(\vec{\xi}))}{\partial n\, \partial n_p} \right] N(\vec{\xi})\, \mathrm{d}S_m, \tag{12d}$$

$$F_+ = \int_S (\beta^+ + \beta^-) G(P, Q(\vec{\xi}))\, \mathrm{d}S + 4\pi \phi_{Sc}(P, X_{Sc}), \tag{12e}$$

$$F_- = \int_S (\beta^+ + \beta^-) \frac{\partial G(P, Q(\vec{\xi}))}{\partial n_p}\, \mathrm{d}S + 4\pi \frac{\partial \phi_{Sc}(P, X_{Sc})}{\partial n_p} + 2\pi \{\beta^+ - \beta^-\}, \tag{12f}$$

where $N(\vec{\xi}) = \{N_1, N_2, \ldots, N_6 \text{ or } N_8\}$ and $\Phi^\pm$ are the column vectors of the velocity potential.

Since the number of collocation points is always greater than the number of nodal points, an overdetermined full matrix is constructed. By using the least-squares procedure, all the unknowns on the surface can be solved.

The implementation of the knife-edge constraint is known to be simple [14]. Consider a thin body discretized into *NNODE* nodal points. *NEDGE* points among them are along the edge, and the number of collocation points is *JMAX*. Then a $JMAX \times 2$ *NNODE* matrix can be constructed by assembling the numerical integration of equations (12a) to (12f). Let Φ_k^+, Φ_k^- be the velocity potentials at the kth nodal point at the knife edge and $\{A_k^+\}$, $\{A_k^-\}$ be the corresponding column matrix. One of Φ_k^+ and Φ_k^- can be replaced by the edge condition of equation 5(c). However, this can be embodied easily by replacing

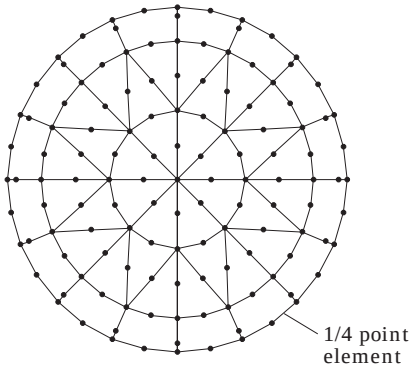

Figure 3. Mesh for a disk problem. (145 nodes and 48 elements)

$\{A_k^+\}$ with $\{A_k^+ + A_k^-\}$ and omitting $\{A_k^-\}$ or vice versa. The final size of the matrix to be calculated is $JMAX \times (2NNODE - NEDGE)$.

5. RESULTS AND DISCUSSION

To verify our present method, firstly, the scattering problem of a plane wave from a rigid circular disk of radius a is tested. The incident velocity potential is given as $\phi_{Sc} = e^{-ikx}$; that is, the normal incident plane wave. For the comparison of the present results with [3], the same mesh with 16 eight-node quadrilateral elements and 32 six-node triangular elements is used, as shown in Figure 3. The calculated non-dimensional wave numbers, ka, are 1, 2, 3, 4 and 5. For the rigid body, the admittances on both surfaces, α^+, α^-, are zero and β^+, β^- are also set to zero. Figure 4 shows the real and imaginary parts of the relative scattered velocity potential on the source side. By comparison with the analytical solution, both results in [3] and the present calculations show excellent agreement. The discrepancies of the two numerical results with the analytical solution near the center of the disk at high frequency, $ka = 5$, are due to the coarseness of the given mesh.

The second case tests the radiation by a vibrating circular disk. The radiation problem has exactly the same solution as for the scattered field. However, the boundary conditions

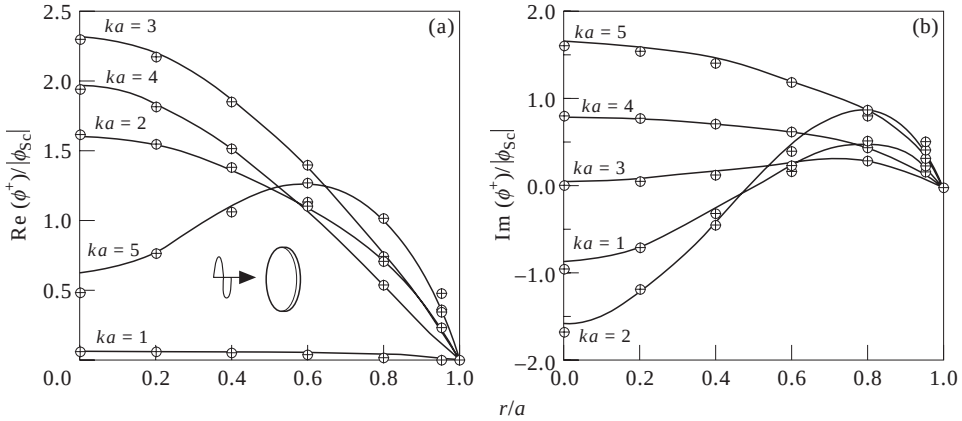

Figure 4. Normalized scattered velocity potential on the illuminated surface. (a) Real term; (b) Imaginary term. ——, analytical solution; −+−, Wu and Wan; −○−, present.

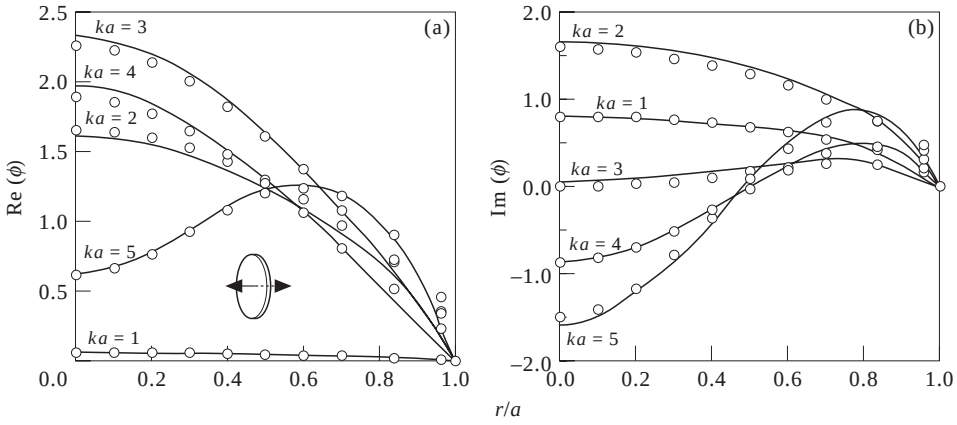

Figure 5. Normalized velocity potential of the vibration circular disk. (a) Real term; (b) imaginary term. ——, analytical solution; ○○○, present.

of the calculation are different for each case. For the scattering problem, α^+, α^-, β^+, β^- are zero; and for the radiation case, α^+, α^- are also zero but β^+, β^- are set equal to the surface-vibrating velocity. The test results are depicted in Figure 5. Good agreement with the analytical solution is again observed. This test partly verifies that the present method can be applied to a thin body with a vibrating surface.

The next problem is the scattering of an incident plane wave from a rigid thin-walled cylinder open at one end. The radius of the open cylinder is a and the length is $2a$. The mesh used to model this open cylindrical shell consists of 40 eight-node quadrilateral elements and eight six-node triangular elements, as shown in Figure 6. Quarter points (filled circles), rather than middle points (open circles), are used for the elements adjacent to the knife edge, which is at the open end of the cylinder. The incident plane wave has a velocity potential of unit amplitude and is assumed to impinge on the cylinder from the open end. The effect of locations of collocation points is shown in Figure 7. Only mesh (b) in Figure 2 is used for the present calculation, and the result is compared with that of Wu and Wan [3]. The difference in the solution is due to the mesh system, as discussed in Figure 2. This result indicates that mesh (a) in Figure 2 should be used for the combined Helmholtz integral equation and mesh (b) for the combined normal derivative integral equation. Figure 8 gives the comparison between the present DBEM, using meshes (a) and (b) in Figure 2 for Equations (6) and (7) respectively, and Wu and Wan's solution for the scattered potentials on both sides (exterior and interior) of the cylindrical surface. The real and imaginary parts of the scattered velocity potentials on the side wall as a function of

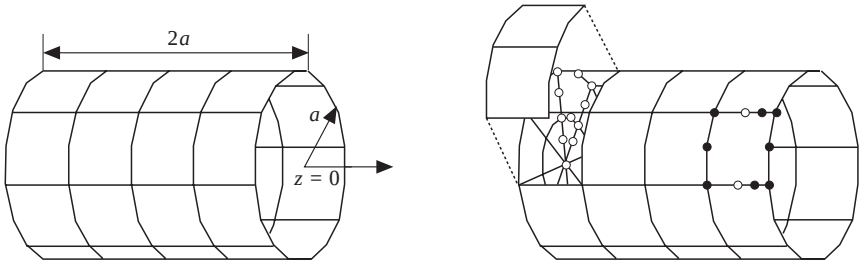

Figure 6. Duct geometry and the used mesh. 40 eight-node quadrilateral and 8 six-node triangular elements are used. (Flooded circle: element for the knife edge, hollow circle: regular element).

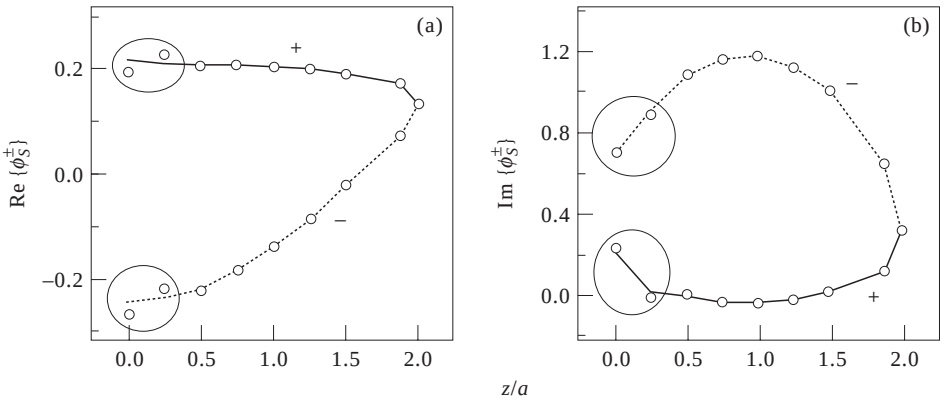

Figure 7. Solid-angle effect at corners and vertexes. Solid and dotted lines represent the results of Wu and Wan's calculation in [3]. Hollow circle is the result by using C^1 element for both equations (6) and (7). Plotted quantity is the scattered velocity potential on the surface of the wall. (a) Real part on the side wall; (b) Imaginary part on the side wall. ○, only using mesh (b) in Figure 2; ——, ····, Wu and Wan [3].

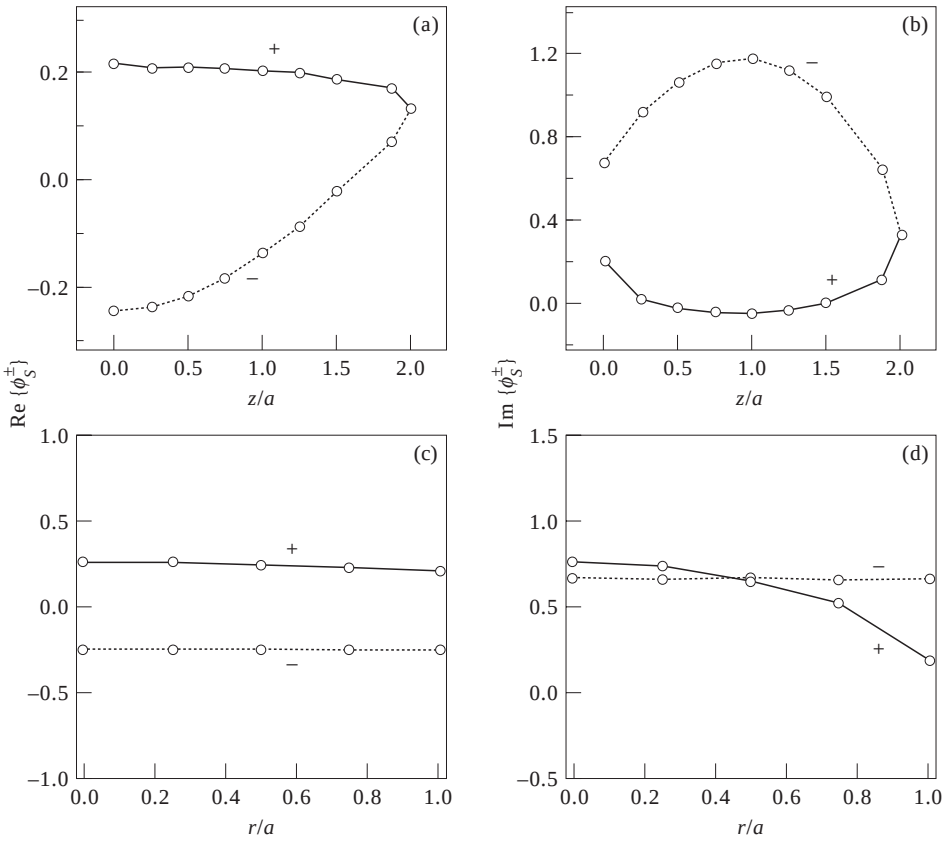

Figure 8. Scattered velocity potential on the wall surface. (a) Real parts on the side wall; (b) Imaginary parts on the side wall; (c) Real parts on the bottom wall; (d) Imaginary parts on the bottom wall. ○, present results; ——, ···· Wu and Wan [3]..

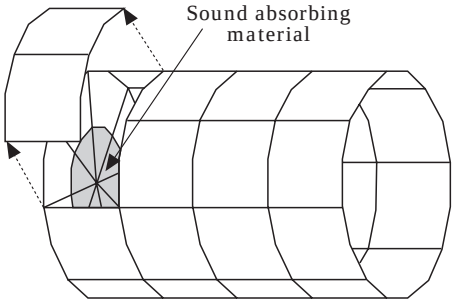

Figure 9. Circular cylindrical shell in which a sound absorbing material is partly mounted inside bottom wall ($\alpha = k^2 3^{-1}(1 + i0{\cdot}3)^{-1}$).

z are shown in Figures 8(a) and (b) respectively. Figure 8(c) shows the real parts of the scattered velocity potentials on the bottom wall as a function of r, and Figure 8(d) shows the corresponding imaginary parts. Again, good agreement is observed. These results indicate that the treatment of the solid angle by the present method is reasonable at the corner or vertex.

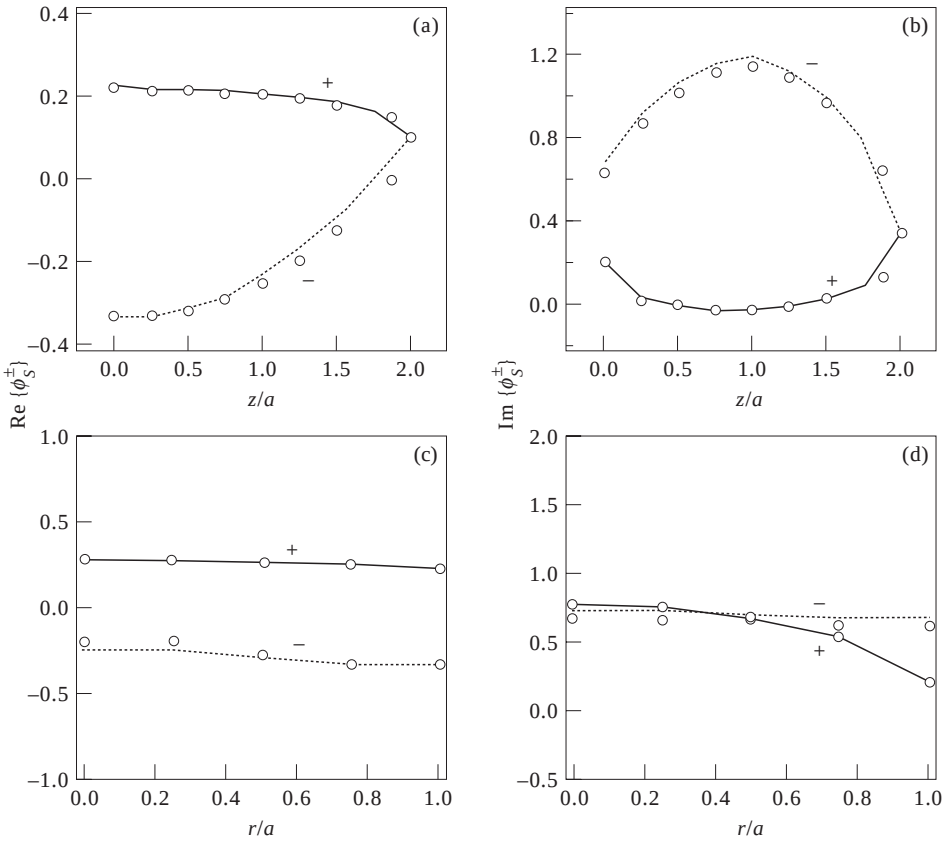

Figure 10. Scattered velocity potential on the wall surface when $ka = 1{\cdot}0$ and the absorbing material with $\alpha = k^2 3^{-1}(1 + i0{\cdot}3)^{-1}$ is partly covered on the inner side of bottom surface ($r = \sqrt{x^2 + y^2}$): (a) Real parts on the side wall; (b) Imaginary parts on the side wall; (c) Real parts on the bottom wall; (d) Imaginary parts on the bottom wall. ○, present results; ——, ····, multi-domain method.

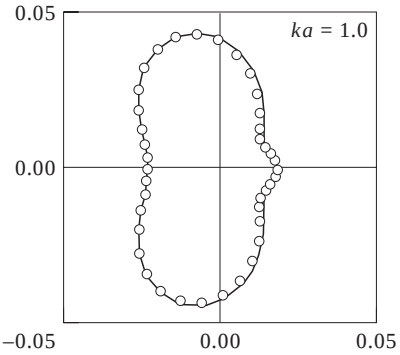

Figure 11. Scattered velocity potential directivity at a distance for $kr = 10{\cdot}0$ from the open end of the duct with absorbing material at $ka = 1{\cdot}0$: solid line, multi-domain method; open circle, present DBEM. ○, present results; —, multi-domain BEM.

Finally, the present DBEM is applied to a thin body having general boundary conditions. The scattering of an incident plane wave from a cylindrical shell open at one end is shown in Figure 9. The inside bottom surface is assumed to be partly coated with an absorbing material. The radius of the coated area is $a/2$ and the coefficient is taken as $\alpha^- = k^2 3^{-1}(1 + \mathrm{i}0{\cdot}3)^{-1}$. The results from the present method are compared with those obtained by the multi-domain method [1]. The scattered velocity potentials on the surface are depicted in Figure 10. Figure 11 is the directivity of the scattered field at $r = 10a$ from the open end of the duct for $ka = 1{\cdot}0$ as in [3]. From the data in Figures 10 and 11, it is seen that the results obtained by the present DBEM and the multi-domain BEM agree well for the cases that have different boundary conditions across the thin body.

6. CONCLUSION

A direct boundary element method (DBEM) is reformulated to extend to thin bodies with rigid and compliant surfaces by removing the normal velocity continuity assumption. The combined Helmholtz integral equation and the combined normal derivative integral equation are solved simultaneously to account for the different boundary conditions on the surfaces across the thin body. The different locations of the collocation points in the two integral equations is critical to cater for the solid angle effect. The knife-edge effect is considered to confirm the knife-edge condition by using quarter-point elements. No fictitious surfaces are required in this formulation. Therefore, the discretization is restricted to the neutral surface of the thin body. The present method can be applied easily to the problem of scattering and radiation from thin bodies of arbitrary shape having either rigid or compliant surfaces.

ACKNOWLEDGMENT

The present work was supported by the Agency for Defense Development.

REFERENCES

1. A. F. Seybert, C. Y. R. Cheng and T. W. Wu 1990 *Journal of the Acoustical Society of America* **88**, 1612–1618. The solution of coupled interior/exterior acoustic problems using the boundary element method.

2. R. Martinez 1991 *Journal of the Acoustical Society of America* **90**, 2728–2738. The thin-shape breakdown (TSB) of the Holmholtz integral equation.
3. T. W. Wu and G. C. Wan 1992 *Journal of the Acoustical Society of America* **92**, 2900–2906. Numerical modeling of acoustic radiation and scattering from thin bodies using a Cauchy principle integral equation.
4. A. W. Maue 1949. *Zeitschrift der Physik* **126**, 601–618. Zur Formulierung eines allgemeinen Beugungsproblems durch eine Integralgleichung.
5. K. M. Mitzner 1966 *Journal of Mathematical Physics* **7**, 2053–2060. Acoustic scattering from an interface between media of greatly different density.
6. M. Tanaka, V. Sladek and S. Sladek 1994 *Applied Mechanics Reviews* **47**, 457–499. Regularization techniques applied to the boundary element method.
7. T. W. Wu 1995 *Journal of the Acoustical Society of America* **97**, 84–91. A direct boundary element method for acoustic radiation and scattering from mixed regular and thin bodies.
8. M. A. Hamdi and J. M. Ville 1986 *Journal of Sound and Vibration* **107**, 231–242. Sound radiation from ducts: theory and experiment.
9. X. F. Wu, A. D. Pierce and J. H. Ginsberg 1987 *IEEE Journal of Oceanic Engineering* **OE-12**, 412–418. Variational method for computing surface acoustic pressure on vibrating bodies, applied to transversely oscillating disks.
10. P. Malbéqui, C. Glandier and C. Reynier 1993 *AIAA Aeroacoustic Conference at Long Beach, CA* **93-4376**. Analysis of sound propagation and radiation in a curved duct using a boundary integral method: comparison with experiment.
11. R. Martinez 1988 *American Institute of Aeronautics and Astronautics Journal* **26**, 396–404. Diffracting open-ended pipe treated as a lifting surface.
12. R. Martinez 1990 *Journal of the Acoustical Society of America* **87**, 523–531. A boundary integral formulation for thin-walled shapes of revolution.
13. T. W. Wu, A. F. Seybert and G. C. Wan 1991 *Journal of the Acoustical Society of America* **90**, 554–560. On the numerical implementation of a Cauchy principal value integral to ensure a unique solution for acoustic radiation and scattering.
14. A. F. Seybert, Z. H. Jia and T. W. Wu 1992 *Journal of the Acoustical Society of America* **91**, 1278–1283. Solving knife-edge scattering problems using singular boundary elements.
15. D. Henshell 1975 *International Journal for Numerical Methods in Engineering* **9**, 495–507. Crack tip finite elements are unnecessary.
16. R. Barsoum 1976 *International Journal for Numerical Methods in Engineering* **10**, 25–37. On the use of isoparametric finite elements in linear fracture mechanics.
17. H. Utsuno, T. W. Wu and A. F. Seybert 1990 *American Institute of Aeronautics and Astronautics Journal* **28**, 1870–1876. Prediction of sound fields in cavities with sound absorbing materials.